Advances in Materials
2015; 4(6): 95-100
Published online November 9, 2015 (http://www.sciencepublishinggroup.com/j/am)
doi: 10.11648/j.am.20150406.11
ISSN: 2327-2503 (Print); ISSN: 2327-252X (Online)

Evaluation of Physical and Structural Properties of Biofield Energy Treated Barium Calcium Tungsten Oxide

Mahendra Kumar Trivedi[1], Rama Mohan Tallapragada[1], Alice Branton[1], Dahryn Trivedi[1], Gopal Nayak[1], Omprakash Latiyal[2], Snehasis Jana[2, *]

[1]Trivedi Global Inc., Henderson, USA
[2]Trivedi Science Research Laboratory Pvt. Ltd., Bhopal, Madhya Pradesh, India

Email address:
publication@trivedisrl.com (S. Jana)

To cite this article:
Mahendra Kumar Trivedi, Rama Mohan Tallapragada, Alice Branton, Dahryn Trivedi, Gopal Nayak, Omprakash Latiyal, Snehasis Jana. Evaluation of Physical and Structural Properties of Biofield Energy Treated Barium Calcium Tungsten Oxide. *Advances in Materials*. Vol. 4, No. 6, 2015, pp. 95-100. doi: 10.11648/j.am.20150406.11

Abstract: Barium calcium tungsten oxide (Ba_2CaWO_6) is known for its double perovskite-type crystal structure. The present study was designed to see the effect of biofield energy treatment on physical, atomic, and structural properties of Ba_2CaWO_6. In this study, Ba_2CaWO_6 powder sample was divided into two parts, one part was remained as untreated, denoted as control, while the other part was subjected to Mr. Trivedi's biofield energy treatment and coded as treated. After that, the control and treated samples were analyzed using X-ray diffraction (XRD), surface area analyzer, Fourier transform infrared (FT-IR), and electron spin resonance (ESR) spectroscopy. The XRD data revealed that the crystallite size was decreased by 20% in the treated Ba_2CaWO_6 sample as compared to the control. The surface area of treated Ba_2CaWO_6 was increased by 9.68% as compared to the control sample. The FT-IR spectroscopic analysis exhibited that the absorbance band corresponding to stretching vibration of W-O bond was shifted to higher wavenumber from 665 cm^{-1} (control) to 673 cm^{-1} after biofield energy treatment. The ESR spectra showed that the signal width and height were decreased by 88.9 and 90.7% in treated Ba_2CaWO_6 sample as compared to the control. Therefore, above result revealed that biofield energy treatment has a significant impact on the physical and structural properties of Ba_2CaWO_6.

Keywords: Ba_2CaWO_6, Biofield Energy Treatment, X-ray Diffraction, Surface Area, Fourier Transform Infrared Spectroscopy, Electron Spin Resonance

1. Introduction

Quaternary perovskites type mixed metal oxides with general formula $A_2MM`O_6$, also known as double perovskites, has 1:1 ordering of the M and M` cations [1]. Recently, these mixed metal oxides with 5d transition metals have attracted a significant attention due to their peculiar electric and magnetic properties. For instance, $Cd_2Re_2O_7$ and $AOsO_6$ (A=K, Cs, Rb) exhibit superconductivity [2-5]. The mixed metal oxides A_2FeReO_6 (A=Ba, Ca, Sr) are ferrimagnetic with high transition temperatures [6, 7]. In addition, for A=Ba and Sr, A_2FeReO_6 are conductors and exhibits negative magnetoresistance effect [8-10]. Similarly, double perovskite-type barium calcium tungsten oxide (Ba_2CaWO_6) is known for its luminance properties and applications in activation of tungsten cathodes for high pressure discharge lamps [11]. Ba_2CaWO_6 has cubic double perovskite structure, where W ions form octahedral crystal structure with oxide ions. In this compound, W atoms are in hexavalent oxidation state *i.e.* W^{+6} with $5d^0$ electronic configuration [12]. Riedel *et al.* had used Ba_2CaWO_6 as activators in tungsten cathode [13]. In order to use Ba_2CaWO_6 in industries, its physical, structural, and atomic properties play a crucial role. Recently, researchers have used various doping techniques to modify the atomic, physical and structural properties of Ba_2CaWO_6. For instance, Yu *et al.* has modified the Ba_2CaWO_6 through doping with Sm^{+3} and Dy^{+3} for orange-red emitting phosphors applications [14]. However, the doping process required very high temperature upto 1200°C in order to get desired properties. Nowadays, the biofield energy treatment has been known as lucrative surrogate approach that may be useful in that concern. The National Center for Complementary and Integrative Health (NCCIH), allows the use of Complementary and Alternative Medicine (CAM) therapies

like biofield energy treatment or healing therapies as an alternative in the healthcare field [15]. Mr. Trivedi's unique biofield energy treatment (The Trivedi effect®) has been extensively studied in the field of material science [16-18]. The biofield energy treatment had significantly altered the atomic, physical and thermal characteristics in several metals [19, 20] and ceramics [21, 22]. After considering the potential impact of biofield energy treatment in materials science, this work was undertaken to evaluate the influence of biofield energy treatment on the atomic, physical, and structural properties of Ba_2CaWO_6 using X-ray diffraction (XRD), surface area analyzer, Fourier transform infrared (FT-IR) spectroscopy, and electron spin resonance (ESR) spectroscopy.

2. Materials and Methods

The Ba_2CaWO_6 powder sample was procured from Sigma Aldrich, USA. The sample was equally divided into two parts. One part was remained as untreated, termed as the control. While, the other part was in sealed pack, handed over to Mr. Trivedi for biofield energy treatment under standard laboratory conditions. Mr. Trivedi provided the treatment through his energy transmission process, without touching the sample and this part was coded as treated. Subsequently, the control and treated Ba_2CaWO_6 samples were characterized using XRD, surface area analyzer, FT-IR, and ESR techniques.

2.1. XRD Study

The XRD analysis of control and treated Ba_2CaWO_6 samples was performed on Phillips, Holland PW 1710 X-ray diffractometer system. The data obtained from the XRD diffractogram in table format, which includes peak position (θ°), peak intensity counts, d value (Å), full width half maximum (FWHM) (θ°), and relative intensity (%) of each peak. The PowderX software was used to compute the lattice parameter and unit cell volume of the control and treated Ba_2CaWO_6 samples. The Scherrer equation was used to compute the crystallite size (G) as following:

$$\text{Crystallite size (G)} = k\lambda/(b\text{Cos}\theta)$$

Here, b is full width half maximum (FWHM) of XRD peaks, k is equipment constant (=0.94), and λ =1.54056 Å.

The percentage change in crystallite size (G) was calculated using following equation:

$$\%\text{ change in crystallite size} = [(G_t-G_c)/G_c] \times 100$$

Where, G_c and G_t are the crystallite size of control and treated Ba_2CaWO_6 powder samples respectively.

2.2. Surface Area Analysis

The Brunauer–Emmett–Teller (BET) surface area analyser, Smart SORB 90 was used to calculate the surface area of the control and treated sample. It has a measuring range of 0.2 m^2/g-1000m^2/g.

2.3. FT-IR Spectroscopy

The FT-IR analysis of control and treated Ba_2CaWO_6 samples were carried out on Shimadzu's FT-IR (Japan) with frequency range of 4000-500 cm^{-1}. The analysis was accomplished to evaluate the effect of biofield treatment on dipole moment, force constant and bond strength in the chemical structure.

2.4. ESR Spectroscopy

The ESR analysis of control and treated Ba_2CaWO_6 samples were performed on Electron Spin Resonance (ESR), E-112 ESR Spectrometer of Varian USA. In this experiment, X-band microwave frequency (9.5 GHz), having sensitivity of 5 x 1010, ΔH spins was used.

3. Results and Discussion

3.1. XRD Study

The XRD technique is a quantitative and non-destructive technique, which is commonly used to study the crystal structure and its parameters of a compound. Figure 1 shows the XRD diffractogram of control and treated samples. The control sample showed the crystalline peaks at Bragg angle (2θ) 18.29°, 30.09°, 35.43°, 43.08°, 43.21°, 53.45°, 53.6°, and 62.75°. These peaks can be indexed to the cubic double perovskite structure Ba_2CaWO_6 according to Joint Committee on Powder Diffraction Standards (JCPDS) file no. 54-0188 [23]. The treated sample also showed similar crystalline peaks with slight alterations in positions. Nevertheless, the crystal structure parameters of control and treated samples were computed using PowderX software. The results are presented in Table 1. The data showed that the lattice parameter and volume of unit cell were slightly reduced in treated samples T1, T2, and T3. However, the lattice parameter and volume of unit cell were slightly increased in treated sample T4. It is reported that the change in temperature caused alterations in the crystal structure properties of Ba_2CaWO_6 [24]. Furthermore, it is possible that the energy transferred through biofield treatment might induce stress in treated Ba_2CaWO_6 samples. Due to this, the internal strain might be generated in the treated samples after biofield energy treatment and that could be responsible for the alteration in the lattice parameter and unit cell volume of Ba_2CaWO_6. Furthermore, the data showed that the density and molecular weight of treated samples were slightly altered as compared to the control. The crystallite size of treated sample was decreased in treated sample T1, though it was not changed in T2, T3 and T4 samples, as compared to the control.

The data exhibited that the crystallite size was decreased from 107.09 nm (control) to 85.68 nm in treated sample (T1). This indicated that crystallite size of treated sample (T1) was reduced by 20% as compared to the control. It is possible that the internal strain, which probably generated through biofield energy treatment might cause fracture in the coarse grain to form sub-grains. Due to this, the crystallite size might be

reduced in the treated sample as compared to the control. It is reported that the crystallite size have strong correlation with the photoluminescence properties of a compound [25]. Thus, based on the alteration in crystallite size in T1, it is assumed that the biofield energy could affect the photoluminescence properties of Ba_2CaWO_6 sample.

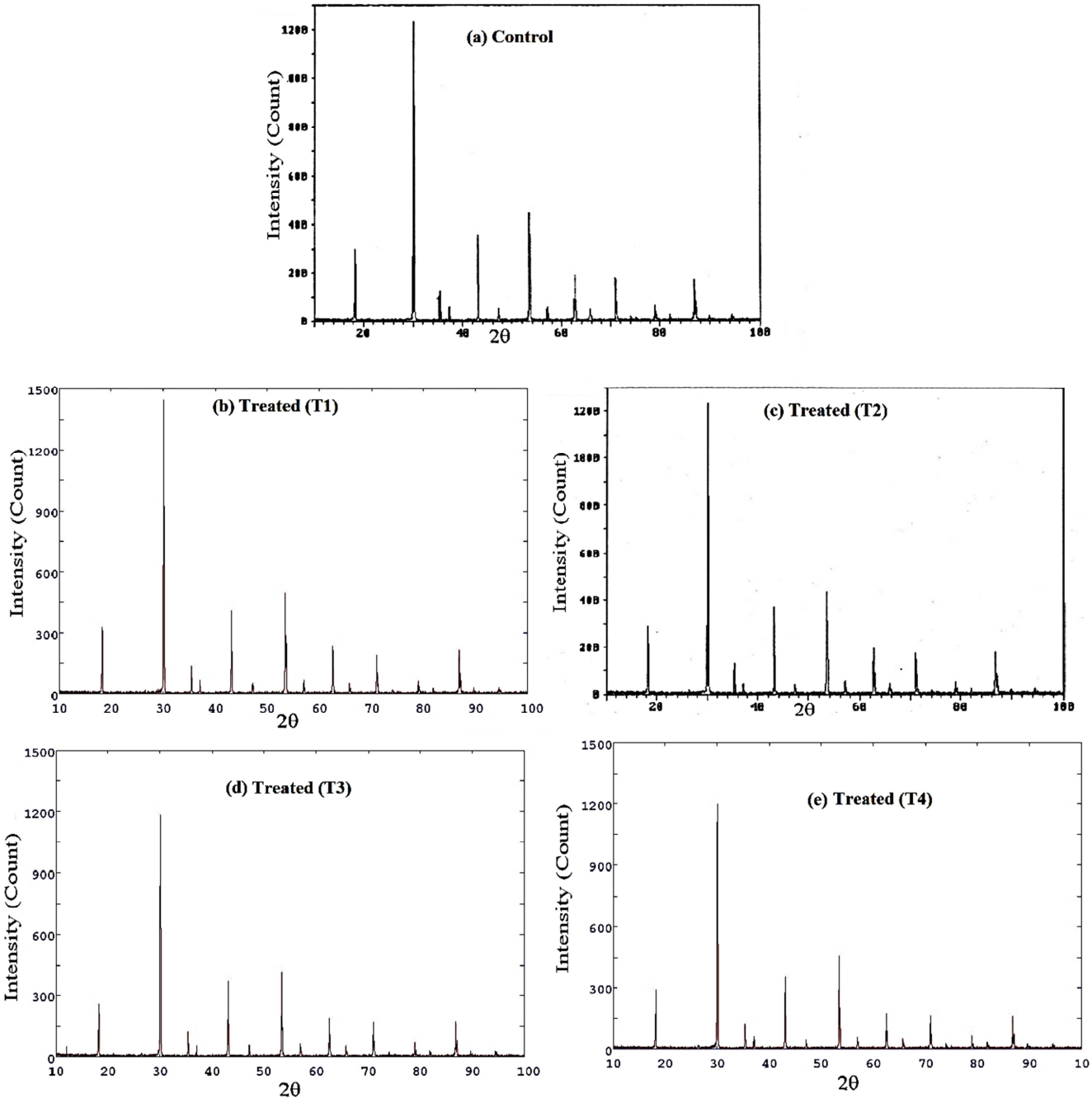

Fig. 1. *X-ray diffractogram of Ba_2CaWO_6 powder.*

Table 1. *Effect of biofield energy treatment on lattice parameter, unit cell volume density atomic weight, and crystallite size of Ba_2CaWO_6 powder.*

Group	Lattice parameter (Å)	Unit cell volume ($\times 10^{-23}$ cm^3)	Density (g/cc)	Molecular weight (g/mol)	Crystallite size (nm)
Control	8.393	59.11	6.731	599.13	107.09
T1	8.388	59.01	6.743	597.67	85.68
T2	8.392	59.09	6.733	598.52	107.09
T3	8.392	59.10	6.733	598.53	107.09
T4	8.396	59.19	6.722	599.52	107.09

3.2. Surface Area Analysis

The surface area analysis of control and treated Ba_2CaWO_6 samples is shown in Table 2. The data showed that the surface area of treated sample was increased from 0.31 m^2/g (control) to 0.34 m^2/g, after biofield treatment. This indicated that the surface area was increased by 9.68% as compared to the control. It was reported that the crystallite size and surface area are inversely proportional to each other [26]. Thus, the increase in surface area of treated Ba_2CaWO_6 was attributed to the decrease in particle size after the biofield treatment. Moreover, the increase in surface area was also supported by a decrease in crystallite size of treated Ba_2CaWO_6 sample after biofield treatment. It is assumed that the biofield energy treatment probably induced the fractures in treated particles and break them down into smaller particles. Due to this, the size of particles might be reduced in the treated sample and that may cause an increase in surface area of treated Ba_2CaWO_6 sample as compared to the control. Furthermore, it is reported that the change in surface area of a compound affects its photoluminescence [27]. Thus, it is presumed that the alteration in surface area in treated Ba_2CaWO_6 might affect its photoluminescence properties.

Table 2. *Surface area analysis of Ba_2CaWO_6 powder.*

Surface Area (m^2/g)		% change
Control	Treated (T1)	
0.31	0.34	9.68

3.3. FT-IR Spectroscopy

Figure 2 shows the FT-IR spectra of control and treated Ba_2CaWO_6 samples. The band observed at 1456 cm^{-1} and 1460 cm^{-1} in control and treated sample, respectively was assigned to –OH bending vibrations. The band observed at 3643 cm^{-1} in control and treated sample was attributed to O-H stretching vibrations [28]. The band found at 665 cm^{-1} with shoulder at 584 cm^{-1} in control, was shifted to 673 cm^{-1} in treated sample. It is reported that the band observed at around 700-600 cm^{-1} in IR spectra was due to W-O stretching vibrations [29]. In addition, the band observed at 810 cm^{-1} with shoulder at 856 cm^{-1} in control, was split into two bands in treated sample at 808 cm^{-1} and 746 cm^{-1}. It can be attributed to internal bonding vibrations of WO_6. Thus, it indicated that the bonding properties of WO_6 probably altered after biofield treatment.

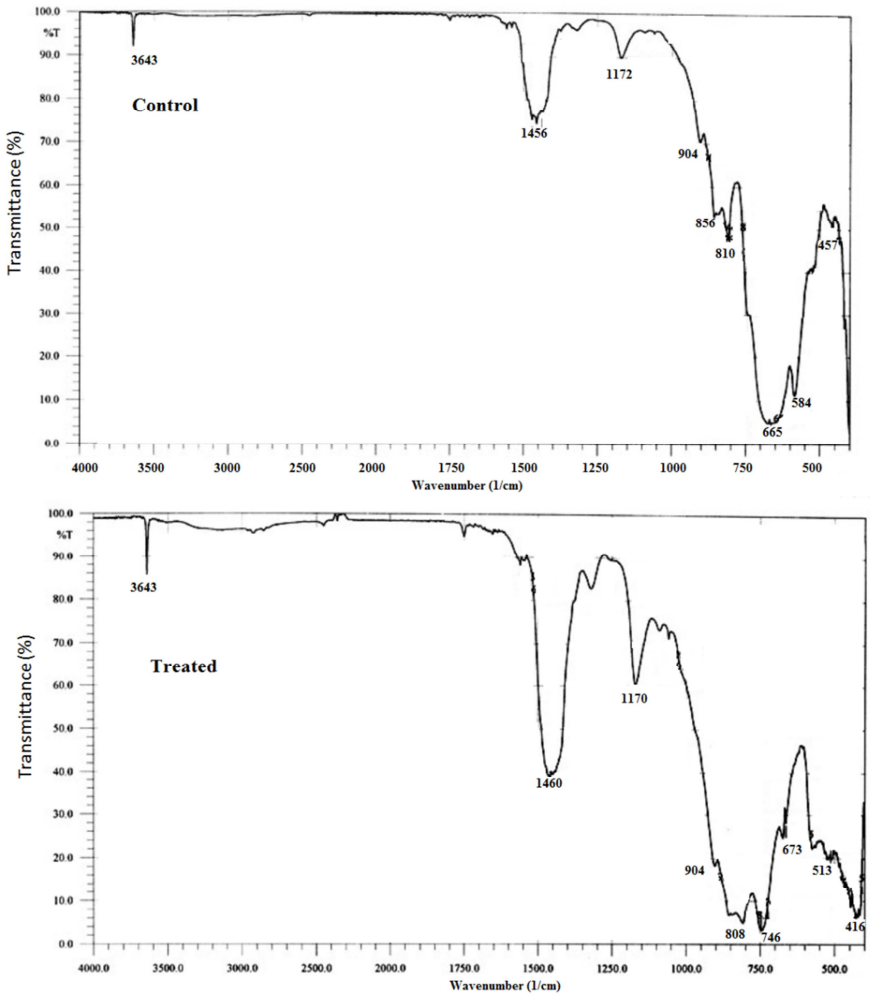

Fig. 2. *FT-IR spectra of Ba_2CaWO_6 powder.*

The wavenumber ($\bar{\nu}$) corresponding to the stretching vibration of a bond is directly related to the bond force constant (k) as follow:

$$\bar{\nu} = \frac{1}{2\pi c}\sqrt{\frac{k}{\mu}}$$

Here, μ is effective mass of atoms, which form the bond and c is the speed of light (3×10^8 m/s). From the above equation, it can be concluded that the change in bond force constant of W-O bond may cause an alteration in wavenumber corresponding to stretching vibration of W-O bond in treated sample as compared to the control. Hence, these data suggested that the biofield energy treatment may influence the bonding properties in Ba_2CaWO_6 and thus bond strength.

3.4. ESR Spectroscopy

The ESR analysis result of control and treated Ba_2CaWO_6 is illustrated in Table 3. The data exhibited the similar g-factor of 2.001 and 2.007 in control and treated sample, respectively. The emergence of ESR signal could be attributed to paramagnetic oxygen ions. However, the ESR signal intensity of treated sample was decreased by 88.9 % as compared to the control. In addition, the ESR signal height of treated Ba_2CaWO_6 was reduced by 90.7% as compared to the control. It is reported that the change in temperature and magnetic susceptibility of ions could alter the intensity and height of the ESR signal [30]. Thus, it is assumed that the biofield energy treatment probably alter the magnetic susceptibility of treated sample as compared to the control.

Table 3. *ESR analysis result of Ba_2CaWO_6 powder.*

Group	g-factor	ESR signal width	ESR signal height
Control	2.0011	90	1.69×10^{-3}
Treated (T1)	2.0073	10	1.56×10^{-4}
Percent Change	0.31	-88.9	-90.7

4. Conclusions

In summary, the biofield energy treatment has a significant impact on the physical and structural properties of Ba_2CaWO_6. The XRD data revealed that the crystallite size of treated Ba_2CaWO_6 was decreased by 20% as compared to the control. The decrease in crystallite size led to increase the surface area of treated Ba_2CaWO_6 by 9.6% as compared to the control. It is assumed that the biofield energy treatment may induced internal strain, due to which the crystallite might fracture and form subgrains. The FT-IR spectroscopy showed that the absorbance band corresponding to stretching vibration of W-O bond was shifted to higher wavenumber from 665 cm^{-1} (control) to 673 cm^{-1} after biofield energy treatment. It could be due to alteration of bonding strength of W-O bond in treated Ba_2CaWO_6 after biofield energy treatment. The ESR showed that the signal width and height were decreased by 88.9 and 90.7% in treated Ba_2CaWO_6 sample as compared to the control. Therefore, it is assumed that biofield energy treatment could be applied to modify the physical and structural properties of Ba_2CaWO_6 for photoluminescence applications.

Acknowledgments

Authors would like to express sincere appreciation to Dr. Cheng Dong of NLSC, Institute of Physics, and Chinese Academy of Sciences, China for permitting us to use Powder-X software. The authors would also like to thank Trivedi Science, Trivedi Master Wellness and Trivedi Testimonials for their support during the work.

References

[1] Fu WT, Au YS, Akerboom S, and Ijdo DJW (2008) Crystal Structures and Chemistry of Double Perovskites $Ba_2M(II)M'(VI)O_6$ (M = Ca, Sr, M'= Te, W, U). J Solid State Chem 181: 2523- 2529.

[2] Hanawa M, Muraoka Y, Tayama T, Sakakibara T, Yamaura J, and Hiroi Z (2001) Superconductivity at 1 K in $Cd_2Re_2O_7$. Phys Rev Lett 87: 187001.

[3] Yonezawa S, Muraoka Y, Matsushita Y, and Hiroi Z (2004) Superconductivity in a pyrochlore-related oxide KOs_2O_6. J Phys Condens Matter 16: L9.

[4] Muramatsu T, Yonezawa S, Muraoka Y, and Hiroi Z (2004) High pressure effects on superconductivity in the β-pyrochlore oxides AOs_2O_6 (A = K, Rb, Cs). J Phys Soc Jpn 73: 2912-2913.

[5] Yonezawa S, Muraoka Y, and Hiroi Z (2004) New β-pyrochlore oxide superconductor $CsOs_2O_6$. J Phys Soc Jpn 73: 1655-1656.

[6] Ward R and Longo J (1960) magnetic phases of the perovskite type. J Am Chem Soc 82: 5958-5958.

[7] Longo J and Ward R (1961) magnetic compounds of hexavalent rhenium with the perovskite-type structure. J Am Chem Soc 83: 2816-2818.

[8] Prellier W, Smolyaninova V, Biswas A, Galley C, Greene RL, Ramesha K et al. (2000) properties of the ferrimagnetic double perovskites A_2FeReO_6 (A = Ba and Ca). J Phys Condens Matter 12: 965.

[9] Abe M, Nakagawa T, and Nomura S (1973) Magnetic and mössbauer studies of the ordered perovskites $Sr_2Fe_1+xRe_1-xO_6$. J Phys Soc Jpn 35: 1360-1365.

[10] Kobayashi KI, Kimura T, Tomioka Y, Sawada H, Terakura K, and Tokura Y (1999) Intergrain tunneling magnetoresistance in polycrystals of the ordered double perovskite Sr_2FeReO_6. Phys rev B 59: 11159.

[11] Capecea AM, Polkb JE, and Shepherda JE (2014) X-ray photoelectron spectroscopy study of $BaWO_4$ and Ba_2CaWO_6. J Electron Spectrosc Relat Phen 197: 102-105.

[12] Bode JHG and Oosterhout ABV (1975) Defect luminescence of ordered perovskites A_2BWO_6. J Lumines 10: 237-242.

[13] Riedel M, Dusterhoft H, and Nagel F (2001) investigation of tungsten cathodes activated with Ba_2CaWO_6. Vacuum 61: 169-173.

[14] Yu R, Noh HM, Moon BK, Choi BC, Jeong JH, Lee HS et al. (2014) Photoluminescence characteristics of Sm^{3+} doped Ba_2CaWO_6 as new orange–red emitting phosphors. J Lumines 152: 133-137.

[15] Barnes PM, Powell-Griner E, McFann K, and Nahin RL (2004) Complementary and alternative Medicine use among Adults: United States, 2002. Adv Data 343: 1-19.

[16] Trivedi MK, Patil S, Tallapragada RM (2013) Effect of bio field treatment on the physical and thermal characteristics of Silicon, Tin and Lead powders J Material Sci Eng 2: 125

[17] Trivedi MK, Patil S, Nayak G, Jana S, Latiyal O (2015) Influence of biofield treatment on physical, structural and spectral properties of boron nitride. J Material Sci Eng 4: 181.

[18] Trivedi MK, Nayak G, Patil S, Tallapragada RM, Latiyal O (2015) Studies of the atomic and crystalline characteristics of ceramic oxide nano powders after bio field treatment. Ind Eng Manage 4: 161.

[19] Trivedi MK, Tallapragada RM, Branton A, Trivedi D, Nayak G, et al. (2015) Potential impact of biofield treatment on atomic and physical characteristics of magnesium. Vitam Miner 3: 129.

[20] Trivedi MK, Nayak G, Patil S, Tallapragada RM, Latiyal O, et al.(2015) An evaluation of biofield treatment on thermal, physical and structural properties of cadmium powder. J Thermodyn Catal 6: 147.

[21] Trivedi MK, Tallapragada RM, Branton A, Trivedi D, Nayak G, et al. (2015) characterization of physical, thermal and structural properties of chromium (VI) oxide powder: Impact of biofield treatment. J Powder Metall Min 4: 128.

[22] Trivedi MK, Nayak G, Patil S, Tallapragada RM, Latiyal O, et al. (2015) Impact of biofield treatment on atomic and structural characteristics of barium titanate powder. Ind Eng Manage 4: 166.

[23] Yu R, Shin DS, Jang K, Guo Y, Noh HM, Moon BK et al. (2014) Luminescence and thermal-quenching properties of Dy^{3+}-doped Ba_2CaWO_6 phosphors. Spectrochim Acta Part A: Mol Biomol Spectrosc 125: 458-462.

[24] Yamamura K, Wakeshima M, and Hinatsu Y (2006) Structural phase transition and magnetic properties of double perovskites Ba_2CaMO_6 (M = W, Re, Os). J Solid State Chem 179: 605-612.

[25] Wang W, Widiyastuti W, Ogi T, Lenggoro IW, and Okuyama K (2007) correlations between crystallite/particle size and photoluminescence properties of submicrometer phosphors. Chem Mater 19: 1723-1730.

[26] Ida J, Honma T, Hayashi S, Nakajima K, Wada E, and Shimizu A (2010) Pressure effect on low-temperature TiO_2 synthesis. J Phys: Conf Series 215: 012132.

[27] Babu KS, Reddy AR, Sujatha C, and Reddy KV (2013) effects of precursor, temperature, surface area and excitation wavelength on photoluminescence of ZnO/mesoporous silica nanocomposite. Ceram Int 39: 3055-3064.

[28] Animitsa IE, Kochetova NA, Denisova TA, Zhuravlev NA, and Baklanova IV (2009) hydration and proton transport in solid solutions based on Ba_2CaWO_6. Russian J Phys Chem 83: 197-202.

[29] Blasse G (1975) vibrational spectra of solid solution series with ordered perovskite structure. J Inorg Nucl Chem 37: 1347-1351.

[30] Häfeli U, Schütt W, Teller J, and Zborowski M (2013) scientific and clinical applications of magnetic carriers. Springer Science & Business Media, Science.